# On the Connectivity of 2-D Random Networks with Anisotropically Radiating Nodes

Justin P. Coon and Carl P. Dettmann

***Abstract*—We study the effect that anisotropic radiation has on the probability that a two-dimensional (2-D) random network is fully connected. To this end, we advance recently established results related to the connectivity of wireless *ad hoc* networks with beamforming – which state that directive transmission can improve connectivity when the path loss exponent is low, and impair connectivity when it is high – by providing a thorough analytical treatment of this topic using a newly established theory of connectivity reported in [1]. Moreover, we exploit our analysis to design optimal radiation patterns in the sense that connectivity is maximized, which can be used as masks to perform antenna pattern synthesis.**

***Index Terms*—Random networks, anisotropic radiation, directivity, full connectivity, antenna pattern synthesis.**

## I. Introduction

Wireless multihop relay network architectures are currently finding use in many infrastructural and *ad hoc* applications. These include emerging energy and utility management scenarios (e.g., "smart grid" and water metering communication networks), industrial wireless sensor networks, and vehicular *ad hoc* networks (VANETs). Even multihop cellular network architectures have been proposed [2], with some solutions being adopted for LTE-Advanced [3].

Many multihop networks possess commonality insomuch as the number and distribution of nodes in the network is often random. A considerable amount of research on random networks has been conducted in the past (see, e.g., [4]–[6]). From a communications perspective, it is of paramount importance to understand the connectivity properties of such networks. This understanding can lead to improved protocols and network deployment methodologies in practice [7].

Most of the work related to network connectivity that can be found in the literature to date has assumed that each node in the network radiates information isotropically. Notable exceptions include [8]–[11]. In particular, simulation studies were carried out in [8], [9] for two-dimensional (2-D) networks to demonstrate that randomized and greedy beamforming approaches improve network connectivity under certain circumstances, while [10], [11] presented semi-analytical results. All of these works focused on uniform linear or circular arrays.

In this paper, we provide further results on the connectivity of dense, 2-D random networks by adopting the network connectivity model recently detailed in [1], [12]. To this end, we study the effect that anisotropic radiation has on network connectivity by explicitly calculating the *connectivity mass* – which measures the likelihood that any given node will connect to another – for several well-known, practical radiation pattern approximations. We conclusively show that, for strict 2-D networks[1], randomized beamforming improves connectivity in networks where the path loss exponent $\eta$ is less than two[2], whereas isotropic radiation is optimal for other cases. Moreover, we exploit our analysis to design optimal radiation patterns in the sense that connectivity is maximized, which can be used as masks to perform antenna pattern synthesis [14].

## II. Anisotropic Connectivity

We consider a network of $N$ nodes located randomly in a two-dimensional space (with volume $V$), and assume the system is homogeneous and isotropic, but where the radiation pattern from each node is anisotropic. The density of the network is given by $\rho = N/V$. In this simplified model, we ignore boundary effects, instead choosing to focus on the connectivity performance in the bulk of the network[3]. However, we note that the model adopted here is representative of certain large networks and those assumed to have periodic boundary conditions, such as indoor networks with access points located along the walls/boundaries.

The probability that any two nodes are directly connected is taken to be the complement of the outage probability with respect to a rate $\mathsf{r}$. For a single-input single-output (SISO) transmission in a Rayleigh fading channel, this probability is given by

$$H = P\left(\log\left(1 + \mathsf{SNR} \cdot X\right) > \mathsf{r}\right) \tag{1}$$

where $X$ is a standard exponential random variable and $\mathsf{SNR}$ denotes the received signal-to-noise ratio. It follows from the Friis transmission formula and numerous experimental path loss studies that

$$\mathsf{SNR} \propto G_T\left(\phi_T - \theta_T\right) G_R\left(\phi_R - \theta_R\right) r^{-\eta} \tag{2}$$

where $G_T\left(\phi_T - \theta_T\right)$ is the gain of the transmit antenna oriented along $\theta_T$ observed in the direction of the receive antenna $\phi_T$, $G_R\left(\phi_R - \theta_R\right)$ is the gain of the receive antenna oriented along $\theta_R$ observed in the direction of the transmit antenna $\phi_R$, $r$ is the distance separating the transmit and

J. P. Coon is with the Telecommunications Research Laboratory, Toshiba Research Europe Ltd., 32 Queen Square, Bristol, BS1 4ND, U.K.; tel: +44 (0)117 906 0700, fax: +44 (0)117 906 0701. (e-mail: justin@toshiba-trel.com). He is also with the Department of Electrical and Electronic Engineering, University of Bristol, BS8 1UB, U.K.

C. P. Dettmann is with the University of Bristol School of Mathematics, University Walk, Bristol, UK, BS8 1TW.

[1] Similar results can be obtained for embedded networks, but this is beyond the scope of this paper.

[2] Low path loss exponents have been reported in numerous propagation studies, particularly in indoor environments (see, e.g., [13]).

[3] Boundary effects in random geometric networks were recently treated in [12].

receive antennas and $\eta$ is the path loss exponent. In a simple line-of-sight (LOS) free space model, we can take $\eta = 2$ and $\phi_R = \phi_T + \pi$. In the following, we will adopt this definition for $\phi_R$ but maintain a general path loss exponent $\eta$. Also, we normalize the radiated (and received) power by enforcing the restriction

$$\int_0^{2\pi} G_T(\phi)\,\mathrm{d}\phi = \int_0^{2\pi} G_R(\phi)\,\mathrm{d}\phi = 2\pi. \tag{3}$$

Now we can further define the pair connectedness function $H$ as

$$H(r,\phi,\theta_T,\theta_R) = \exp\left(-\frac{\beta r^\eta}{G_T(\phi-\theta_T)\,G_R(\phi+\pi-\theta_R)}\right) \tag{4}$$

where $\beta$ defines the length scale. For the standard case of isotropic radiation, $G_T = G_R = 1$ for $0 \le \phi \le 2\pi$. In this case, we can apply the theory detailed in [12] to obtain an accurate analysis of the probability that the network is fully connected. We can choose many other radiation gain patterns to better represent realistic propagation models; however, before doing so, we give further details of the network connectivity model in a generalized manner.

From [12], we know that the first order full connection probability for the network is

$$P_{fc} \approx 1 - Ne^{-\rho M} \tag{5}$$

where

$$M = \frac{1}{2\pi}\int rH(r,\phi,\theta_T,\theta_R)\,\mathrm{d}r\mathrm{d}\phi\mathrm{d}\theta_R \tag{6}$$

is called the *connectivity mass*. The factor of $1/(2\pi)$ is included in this expression for normalizing the orientation angle $\theta_R$. The orientation of the transmitter is arbitrary since the system is isotropic, so we take it to be $\theta_T = 0$. Thus, the connectivity mass can be rewritten as

$$\begin{aligned} M &= \frac{\Gamma\left(\frac{2}{\eta}\right)}{2\pi\eta\beta^{\frac{2}{\eta}}}\int \left(G_T(\phi)\,G_R(\phi+\pi-\theta)\right)^{\frac{2}{\eta}}\mathrm{d}\theta\mathrm{d}\phi \\ &= \frac{\Gamma\left(\frac{2}{\eta}\right)}{2\pi\eta\beta^{\frac{2}{\eta}}}\left(\int_0^{2\pi} G_T(\phi)^{\frac{2}{\eta}}\mathrm{d}\phi\right)\left(\int_0^{2\pi} G_R(\phi)^{\frac{2}{\eta}}\mathrm{d}\phi\right) \end{aligned} \tag{7}$$

where $\Gamma(x)$ is the gamma function and the second equality follows from the fact that the gain functions are periodic in their argument. Now we examine some simple but practical functions for $G_T$ and $G_R$.

### A. Isotropic Radiation

As a benchmark, we set $G_T = G_R = 1$ for $0 \le \phi \le 2\pi$. This is representative of a dipole radiation pattern along the azimuth plane (i.e., in 2-D). In this case, we have

$$M_{iso} = \frac{2\pi\Gamma\left(\frac{2}{\eta}\right)}{\eta\beta^{\frac{2}{\eta}}}. \tag{8}$$

### B. Cardioid Pattern

A simple but practical radiation pattern that one might consider is the cardioid, which is given by

$$G_T(\phi) = G_R(\phi) = 1 + \cos\phi, \quad 0 \le \phi \le 2\pi. \tag{9}$$

This function well-approximates the radiation pattern exhibited by a patch antenna in a plane [15]. In this case, we can write

$$\begin{aligned} M_{car} &= \frac{\Gamma\left(\frac{2}{\eta}\right)}{2\pi\eta\beta^{\frac{2}{\eta}}}\left(\int_0^{2\pi}(1+\cos\phi)^{\frac{2}{\eta}}\mathrm{d}\phi\right)^2 \\ &= \left(\frac{4}{\beta}\right)^{\frac{2}{\eta}}\frac{\Gamma\left(\frac{1}{2}+\frac{2}{\eta}\right)^2}{\Gamma\left(1+\frac{2}{\eta}\right)}. \end{aligned} \tag{10}$$

This function is well behaved for typical values of $\beta$ and $\eta$, and we note that $M_{iso} = M_{car}$ at $\eta = 2$.

### C. Directed Transmission

For a directed transmission, such as that generated by an end-fire array, we may approximate the main lobe of the gain functions by [15, pg. 46]

$$G_T(\phi) = G_R(\phi) = \begin{cases} \lambda\pi\cos(\lambda\phi), & -\frac{\pi}{2\lambda} \le \phi \le \frac{\pi}{2\lambda} \\ 0, & \text{otherwise} \end{cases} \tag{11}$$

where $\lambda \ge 1$ defines the directivity of the beam, with larger $\lambda$ indicating a higher degree of directivity. Now we have

$$\begin{aligned} M_{dir} &= \frac{\Gamma\left(\frac{2}{\eta}\right)}{2\pi\eta\beta^{\frac{2}{\eta}}}\left(\int_0^{2\pi}(\lambda\pi\cos(\lambda\phi))^{\frac{2}{\eta}}\mathrm{d}\phi\right)^2 \\ &= \left(\frac{\pi^2\lambda^{2-\eta}}{\beta}\right)^{\frac{2}{\eta}}\frac{\eta\Gamma\left(\frac{1}{2}+\frac{1}{\eta}\right)^2}{2B\left(\frac{1}{\eta},\frac{1}{\eta}\right)} \end{aligned} \tag{12}$$

where $B(x,y)$ is the beta function. Again, we note that $M_{dir} = M_{iso} = M_{car}$ at $\eta = 2$.

Equation (5) illustrates a simple one-to-one relationship between the connectivity mass $M$ and the full connection probability $P_{fc}$ at high node densities. Thus, it is of interest to view $M$ as a function of the path loss exponent $\eta$ for various radiation patterns. Fig. 1 provides such an illustration for the three patterns discussed above. We see that directive transmission yields a higher connectivity mass, and thus an exponentially greater probability of the network being fully connected, for environments that exhibit good path loss properties, corresponding to $\eta < 2$. Conversely, isotropic radiation yields the best connectivity characteristics for $\eta > 2$.

These results are generally in line with the numerical results presented in [11], but where the threshold value of the path loss exponent is two instead of three. This result simply follows from the fact that we consider strict 2-D networks here, and from the normalization defined by (3). One benefit of our approach compared to that presented in [11] is that our analysis is based on the fundamental principle of the connectivity mass, which can be calculated for *general* antenna gain models and applied to the complete theory outlined in [12], whereas [11] is largely restricted to uniform circular arrays. Furthermore, the

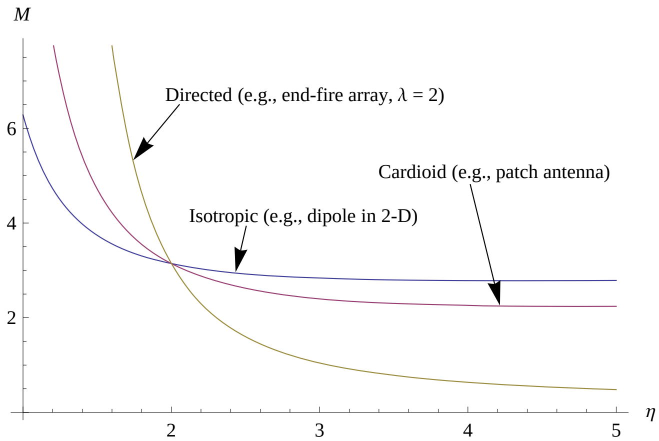


Fig. 1. Illustration of the connectivity masses corresponding to different radiation patterns, plotted as a function of the path loss exponent $\eta$.

results presented in [11] are somewhat numerical, in contrast to the explicit analytical expressions detailed in this paper. In fact, the quantitative approach that we have taken not only yields specific rules rather than general guidelines on network connectivity performance, but facilitates the optimization of antenna patterns and physical element/array geometries, as discussed in the next section.

## III. Stationary Radiation Patterns

In the discussion above, we considered a few different radiation patterns. From that discussion, the question of pattern optimality naturally arises. In particular, since we want to maximize the connectivity mass $M$ as defined in (7), it follows that we should let $G_T = G_R = G$, and seek the path $G(\phi)$ that maximizes the functional

$$S[G] = \int_0^{2\pi} G(\phi)^{\frac{2}{\eta}} \,\mathrm{d}\phi \tag{13}$$

subject to the constraint

$$\int_0^{2\pi} G(\phi)\,\mathrm{d}\phi = 2\pi. \tag{14}$$

### A. Single Sector Radiation

In the first instance, we consider a simplified sectorized radiation model. For this case, let us define $G(\phi) \geq 0$ on the interval $\phi \in \left[-\frac{\pi}{2\lambda}, \frac{\pi}{2\lambda}\right]$ for some $\lambda \leq 1/2$, and $G(\phi) = 0$ elsewhere. We can find the stationary paths of $S[G]$ by employing the tools of the calculus of variations. In this case, we formulate the Lagrangian $L(\phi, G, \xi) = G^{\frac{2}{\eta}} - \xi G$, where $\xi$ is the Lagrange multiplier. Solving the Euler-Lagrange equation $\partial L/\partial G = 0$ and using the constraint (14) yields the stationary path

$$G(\phi) = 2\lambda, \quad -\frac{\pi}{2\lambda} \leq \phi \leq \frac{\pi}{2\lambda}. \tag{15}$$

It remains to determine whether this path is an extremal, i.e., whether it yields a minimum or maximum of $S$. This is easily determined by calculating the second variation $\Delta_2[G,h]$ for some admissible path $h$, which yields

$$\begin{aligned}\Delta_2[G,h] &= \int_{-\frac{\pi}{2\lambda}}^{\frac{\pi}{2\lambda}} \frac{\partial^2 L}{\partial G^2} h(\phi)^2 \,\mathrm{d}\phi \\ &= \frac{2}{\eta}\left(\frac{2}{\eta}-1\right)(2\lambda)^{\frac{2}{\eta}-2} \int_{-\frac{\pi}{2\lambda}}^{\frac{\pi}{2\lambda}} h^2 \mathrm{d}\phi. \end{aligned} \tag{16}$$

It follows that $\Delta_2[G,h] > 0$ if $\eta < 2$ and $\Delta_2[G,h] < 0$ if $\eta > 2$. We already know that all paths $G$ lead to identical connectivity masses for $\eta = 2$ due to the constraint on the area under $G$ (i.e., the power normalization). Thus, we readily conclude that the path defined in (15) is a maximum for $\eta > 2$ and a minimum for $\eta < 2$.

A corollary is that isotropic radiation ($\lambda = 1/2$) is optimal with respect to connectivity when $\eta > 2$. Moreover, single-sector directed transmission provides a lower bound on the connectivity mass for $\eta < 2$. Indeed, one can easily find radiation patterns that yield better connectivity in this case, and in fact there is no upper bound; one may obtain arbitrarily good connectivity by designing the beam width to be as small as possible. An important conclusion from this brief analysis is that connectivity in random networks operating in low path loss environments is dictated by the physical limitations of the antenna geometries and device properties.

### B. Antenna Pattern Synthesis

In practical networks, it may not be desireable (or possible) to design radiation patterns to be sectorized as discussed in the previous section. Indeed, when the side lobes are significantly smaller than the main lobe of an antenna radiation pattern, medium access control protocols often perform poorly due to the hidden node phenomenon. Thus, it is of interest to synthesize an antenna pattern for each node in the network subject to certain constraints such that the probability of a network being fully connected is maximized.

We may extend the discussion above to patterns that occupy the entire polar plane. To this end, let

$$G(\phi) = \begin{cases} G_1(\phi), & \phi \in \mathcal{R}_1 \\ \vdots & \\ G_n(\phi), & \phi \in \mathcal{R}_n \end{cases} \tag{17}$$

where $\mathcal{R}_i \subset [0, 2\pi)$, with $\mathcal{R}_i \cap \mathcal{R}_j = \emptyset$ for $i \neq j$ and $\bigcup_i \mathcal{R}_i = [0, 2\pi)$. Suppose the average power radiated in $\mathcal{R}_i$ is constrained by

$$\int_{\mathcal{R}_i} G_i(\phi)\,\mathrm{d}\phi = P_i, \quad i = 1, \ldots, n \tag{18}$$

with $\sum_i P_i = 2\pi$. A function $G(\phi)$ that adheres to this definition may form a mask for antenna pattern synthesis in practice [14].

Now, we wish to find the set of paths $\{G_i\}$ that maximize the functional

$$S[G_1, \ldots, G_n] = \sum_{i=1}^{n} \int_{\mathcal{R}_i} G_i(\phi)^{\frac{2}{\eta}} \,\mathrm{d}\phi. \tag{19}$$

Given the constraints defined in (18), this amounts to maximizing the set of functionals given by

$$\left\{ S\left[G_i\right] = \int_{\mathcal{R}_i} G_i\left(\phi\right)^{\frac{2}{\eta}} \,\mathrm{d}\phi \right\}. \tag{20}$$

We take the regions $\{\mathcal{R}_i\}$ and the power levels $\{P_i\}$ to be constant, but these can be treated as design parameters that can be used for further optimization as will be shown below.

It follows from the Euler-Lagrange formulae for these functionals that

$$G_i\left(\phi\right) = \left(\frac{\eta}{2}\xi_i\right)^{\frac{1}{\frac{2}{\eta}-1}}, \quad \phi \in \mathcal{R}_i \tag{21}$$

for $i = 1, \ldots, n$ where $\{\xi_i\}$ are Lagrange multipliers. Using the constraints (18), we arrive at the following explicit definition for the stationary paths $\{G_i\}$:

$$G_i\left(\phi\right) = \frac{P_i}{|\mathcal{R}_i|}, \quad \phi \in \mathcal{R}_i;\, i = 1, \ldots, n. \tag{22}$$

It follows that

$$S\left[G_1, \ldots, G_n\right] = \sum_{i=1}^{n} P_i^{\frac{2}{\eta}} \left|\mathcal{R}_i\right|^{1-\frac{2}{\eta}} = 2\pi \sum_{i=1}^{n} r_i \left(\frac{p_i}{r_i}\right)^{\frac{2}{\eta}} \tag{23}$$

on the stationary paths, where $p_i = P_i/\left(2\pi\right) \in [0,1]$ and $r_i = \left|\mathcal{R}_i\right|/\left(2\pi\right) \in [0,1]$. Again, we can calculate the second variation to see that $S$ is a maximum if $\eta > 2$ and a minimum if $\eta < 2$.

This analysis provides rules on antenna pattern synthesis that can be followed to ensure the connectivity is maximized for a given $\eta$. Of course, the analysis shows that, for the case where $\eta < 2$, there is no theoretical upper bound on the connectivity mass since one may choose $|\mathcal{R}_i|$ as small as one likes for some $i$.

For the case where $\eta > 2$, we have the bound

$$S \leq 2\pi \left(\sum_{i=1}^{n} r_i \frac{p_i}{r_i}\right)^{\frac{2}{\eta}} = 2\pi \tag{24}$$

which follows from the power mean inequality

$$\left(\sum_{i=1}^{n} w_i x_i^a\right)^{\frac{1}{a}} \leq \left(\sum_{i=1}^{n} w_i x_i^b\right)^{\frac{1}{b}} \tag{25}$$

where $\sum_i w_i = 1$ and $a < b$. Now suppose we specify the set $\{P_i\}$, and then design the set $\{\mathcal{R}_i\}$ to maximize $S$, or *vice versa*. Following this approach, the bound given in (24) can be attained by letting $r_i = p_i$ for all $i$, which is just isotropic radiation. This result coincides with that given for a single sector radiation pattern discussed in III-A.

## IV. Conclusions

In this contribution, we studied the effect that antenna directivity has on the connectivity properties of dense, 2-D random networks. Our analysis was framed within the network connectivity model detailed in [12]. We calculated the connectivity mass related to various radiation patterns, and showed that isotropic radiation is optimal with respect to connectivity when the path loss exponent is greater than two, but single-sector directed transmission yields superior performance for other cases. Moreover, we designed optimal radiation patterns using our analysis, which can be used as masks to perform antenna pattern synthesis in practical systems.

## Acknowledgment

The authors wish to thank the directors of Toshiba TRL for their continued support.

## References

[1] J. Coon, C. Dettmann, and O. Georgiou, “Impact of boundaries on fully connected random geometric networks,” *Phys. Rev. E*, vol. 85, p. 011138, Jan 2012. [Online]. Available: http://link.aps.org/doi/10.1103/PhysRevE.85.011138

[2] Y. Lin and Y. Hsu, “Multihop cellular: a new architecture for wireless communications,” in *INFOCOM 2000. Nineteenth Annual Joint Conference of the IEEE Computer and Communications Societies*, vol. 3, 2000, pp. 1273–1282.

[3] M. Baker, “From LTE-advanced to the future,” *IEEE Commun. Mag.*, vol. 50, no. 2, pp. 116–120, 2012.

[4] P. Balister, A. Sarkar, and B. Bollobás, “Percolation, connectivity, coverage and colouring of random geometric graphs,” *Handbook of Large-Scale Random Networks*, pp. 117–142, 2008.

[5] M. Haenggi, J. Andrews, F. Baccelli, O. Dousse, and M. Franceschetti, “Stochastic geometry and random graphs for the analysis and design of wireless networks,” *IEEE J. Sel. Areas Commun.*, vol. 27, no. 7, pp. 1029–1046, 2009.

[6] J. Li, L. Andrew, C. Foh, M. Zukerman, and H. Chen, “Connectivity, coverage and placement in wireless sensor networks,” *Sensors*, vol. 9, no. 10, pp. 7664–7693, 2009.

[7] V. Ravelomanana, “Extremal properties of three-dimensional sensor networks with applications,” *IEEE Trans. Mobile Computing*, vol. 3, no. 3, pp. 246–257, 2004.

[8] C. Bettstetter, C. Hartmann, and C. Moser, “How does randomized beamforming improve the connectivity of ad hoc networks?” in *Communications, 2005. ICC 2005. IEEE International Conference on*, vol. 5, Seoul, Korea, May 2005, pp. 3380–3385.

[9] X. Zhou, H. Jones, S. Durrani, and A. Scott, “Effect of beamforming on the connectivity of ad hoc networks,” in *Proc. AusCTW*, Adelaide, Australia, Feb. 2007, pp. 13–18.

[10] H. Koskinen, “Analytical study of connectivity in wireless multihop networks utilizing beamforming,” in *Proceedings of the 9th ACM/IEEE International Symposium on Modeling Analysis and Simulation of Wireless and Mobile Systems*, Torremolinos, Spain, Oct. 2006, pp. 212–218.

[11] X. Zhou, S. Durrani, and H. Jones, “Connectivity analysis of wireless ad hoc networks with beamforming,” *IEEE Trans. Veh. Technol.*, vol. 58, no. 9, pp. 5247–5257, Nov. 2009.

[12] J. Coon, C. Dettmann, and O. Georgiou, “Full connectivity: corners, edges and faces,” *Journal of Statistical Physics*, vol. 147, no. 4, pp. 758–778, 2012.

[13] S. Y. Seidel and T. S. Rappaport, “914 MHz path loss prediction models for indoor wireless communications in multifloor buildings,” *IEEE Trans. Antennas Propag.*, vol. 40, no. 2, pp. 207–217, Feb. 1992.

[14] G. Collin, E. Géron, J. Lucas, and T. Ditchi, “Fast antenna pattern synthesis using the variational method,” *IET Microwaves, Antennas & Propagation*, vol. 4, no. 11, pp. 1689–1697, 2010.

[15] C. Balanis, *Antenna Theory: Analysis and Design*, 2nd ed. J. Wiley, New York, 1997.